Supporting Information for

Modeling Dynamic Swelling of Polymer-Based Artificial Muscles

Shefik Bowen[1], Daniel Hallinan[1,*]

[1]Florida A&M University-Florida State University (FAMU-FSU) College of Engineering, Department of Chemical & Biomedical Engineering and Aero-propulsion, Mechatronics, and Energy Center, Tallahassee, FL 32310.

*Corresponding author email: dhallinan@eng.famu.fsu.edu

Derivation of relationship between total molar concentration and volume fractions

The total molar concentration is initially equal to the polymer concentration for a dry polymer

$$C(0) = C_2$$

As presented in the main manuscript, the molar concentration of any species, i, is equal to its volume fraction divided by the molar volume of the species.

$$C_i = \frac{\phi_i}{v_i}$$

For the dry polymer, $\phi_2 = 1$, and thus

$$C(0) = \frac{\phi_2}{v_2} = \frac{1}{v_2}$$

At long time, the polymer network is swollen to equilibrium by the solvent and the total concentration is

$$C(\infty) = C_1 + C_2 = \frac{\phi_1}{v_1} + \frac{\phi_2}{v_2}$$

Volume fractions sum to one, such that $\phi_2 = 1 - \phi_1$, and

$$C(\infty) = \frac{\phi_1}{v_1} + \frac{1}{v_2} - \frac{\phi_1}{v_2}$$

Recalling that $C(0) = \frac{1}{v_2}$,

$$C(\infty) - C(0) = \frac{\phi_1}{v_1} - \frac{\phi_1}{v_2}$$

Description of relationship between total mass concentration and volume fractions

Because $\rho_s = \frac{M_s}{V_s}$, the mass reported in Satterfield' s work from 2008 can be related to our calculations by the density of the solvent.

$M(t) - M_o = M_s$ and $V_f = M_\infty/\rho_{total} = M_s/\rho_s + M_p/\rho_p$

The denominator is the final volume of solvent. Assuming volume additivity, if the final volume of solvent is merely the total volume minus the polymer volume, the relation is simply $\frac{\frac{M(t)-M_0}{\rho_s}}{\left(\frac{M_s}{\rho_s}+\frac{M_o}{\rho_p}\right)-\frac{M_o}{\rho_{polymer}}} = \frac{V(t)-V_i}{V_f-V_i} = \frac{R(t)^3-R_i^3}{R_f^3-R_i^3}$.

Longer-time Cartesian Simulation

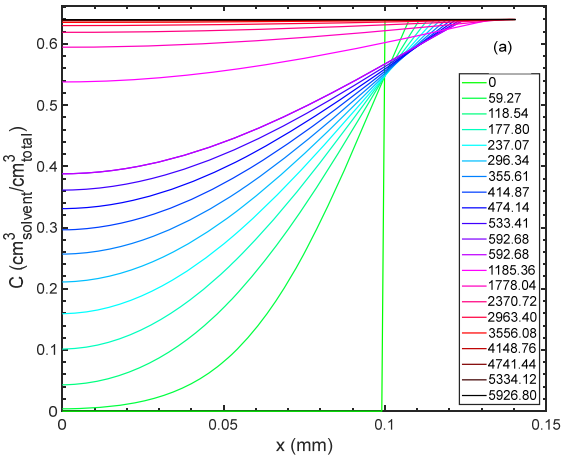

Figure S1. Concentration profiles from a simulation in Cartesian coordinates equivalent to Figure 2 but run to $Time_{final}$. This simulation is run to sufficiently long time that a flat equilibrium profile (black line) is achieved at 5926.80 s. The specific time in seconds for each concentration profile were chosen for convenient graphical representation and are reported in the legend. At early times there is a 59.27 second time increment whereas after longer times, the increment becomes 592.7 seconds.

Parameter Values from Literature

Table S1. Sample polymer solvent systems and reported diffusion coefficients, χ parameter, calculated coil strain, and work done. Polyurethane (PU), Nitrile Butadiene Rubber (NBR), Neoprene (NP), styrene butadiene rubber (SBR), ethylene propylene diene terpolymer (EPDM), carbon fiber/polydimethylsiloxane (CF/PDMS), carbon nanotube/ silicon yarn (CNT/SY), sulphonated poly(ether ether keytone)(SPEEK) at 25 $°C$.[1-3]

Polymer-Solvent System	Solvent	Diffusion Coefficient $D \times 10^7 \frac{cm^2}{s}$	χ parameter	Equilibrium Swelling Ratio	Actuation %	Work (J/kg)
This Work	Water	1	0.56	2.77	81	1.1
CNT	-	-	-	-	7	-
CNT/SY	-	-	-	-	60	836
CF/PDMS	-	-	-	-	50	758
PU	Hexane	1.114	1.135	-	-	-
PU	Heptane	1.024	1.292	-	-	-
PU	Octane	0.859	1.971	-	-	-
PU	Nonane	0.709	1.438	-	-	-
PU	Decane	0.637	1.628	-	-	-
NBR	Benzene	4.21	-	-	-	-
NBR	Toluene	5.02	-	-	-	-
NBR	p-Xylene	1.69	-	-	-	-
NBR	Mesitylene	1.04		69.2		
NBR	Anisole	3.15	-	-	-	-
CR	Benzene	6.14	-	-	-	-
CR	Toluene	7.31	-	-	-	-
CR	p-Xylene	3.60	-	-	-	-
CR	Mesitylene	2.74	-	-	-	-
CR	Anisole	4.41	-	-	-	-
SBR	Benzene	9.71	-	-	-	-
SBR	Toluene	7.89	-	-	-	-
SBR	p-Xylene	2.42	-	-	-	-
SBR	Mesitylene	3.43	-	-	-	-
SBR	Anisole	5.39	-	-	-	-

EPDM	Benzene	6.27	-	61.5	-	-
EPDM	Toluene	6.69	-	63.7	-	-
EPDM	p-Xylene	7.10	-	64.2	-	-
EPDM	Mesitylene	3.79	-	64.6	-	-
EPDM	Anisole	4.89	-	63.7	-	-
NR	Benzene	9.89	-	-	-	-
NR	Toluene	10.22	-	-	-	-
NR	p-Xylene	5.04	-	-	-	-
NR	Mesitylene	3.47	-	61.3	-	-
NR	Anisole	3.20	-	-	-	-
CR	Mesitylene	-	-	65.4	-	-
SBR	Mesitylene	6.75	-	61.4	-	-
EPDM	Mesitylene	5.98	-	62.9	-	-
NR	Mesitylene	5.63	-	61.3	-	-
SPEEK	Methyl ethyl ketone	-	2.584	-	-	-
SPEEK	Acetone	-	2.068	-	-	-
SPEEK	Acetic acid	-	0.874	-	-	-
SPEEK	Methylamine	-	0.564	-	-	-
SPEEK	1-Butanol	-	1.621	-	-	-
SPEEK	Cyclohexanol	-	0.732	-	-	-
SPEEK	2-Propanol	-	0.939	-	-	-
SPEEK	1,5-Pentanediol	-	1.208	-	-	-
SPEEK	1-Propanol	-	1.473	-	-	-
SPEEK	Formic acid	-	−0.399	-	-	-
SPEEK	1,4-Butanediol	-	0.802	-	-	-

SPEEK	1,3-Propanediol	-	1.363	-	-	-
SPEEK	Ethanol	-	1.14	-	-	-
SPEEK	Methanol	-	1.333	-	-	-
SPEEK	Ethylene glycol	-	−0.352	-	-	-
SPEEK	Glycerol	-	4.694	-	-	-
SPEEK	Formamide	-	−0.179	-	-	-
SPEEK	Water	-	1.435	-	-	-

Twisting and Coiling

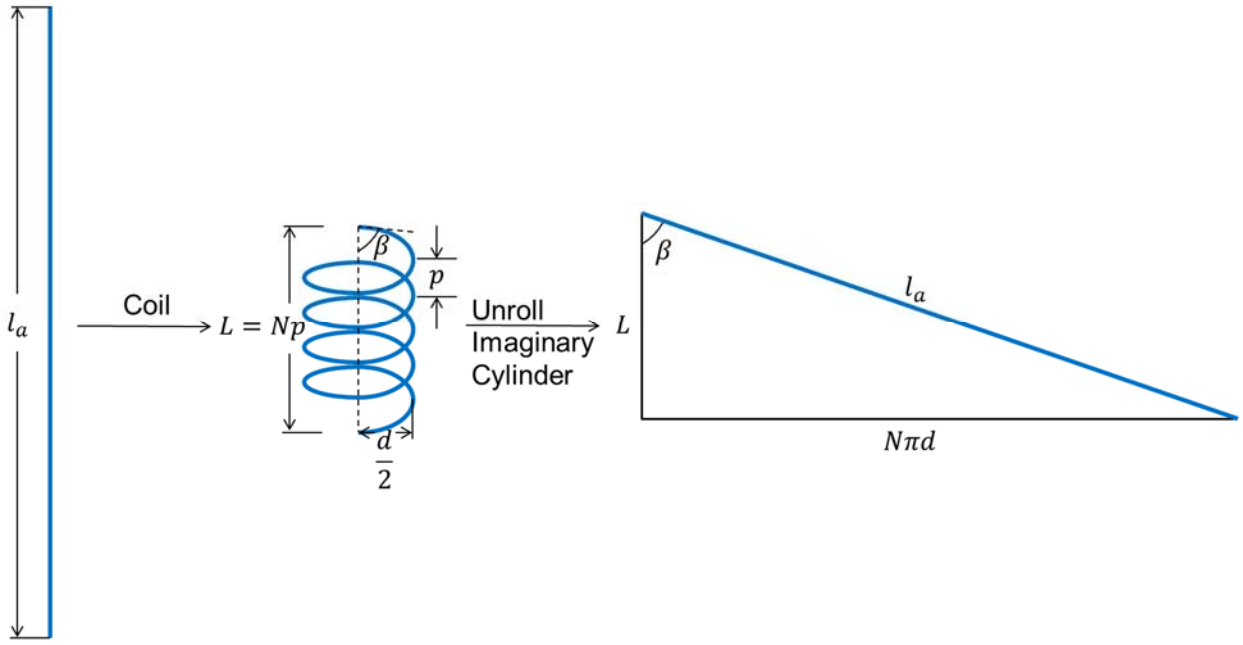

Figure S2. Schematics (not to scale) depicting geometry of coiled fiber.

As shown in Figure S1, there is a simple geometric relationship between the fiber length, l_a, and the coil length, L, defined by the coil bias angle, β, i.e. $L = l_a cos(\beta)$.

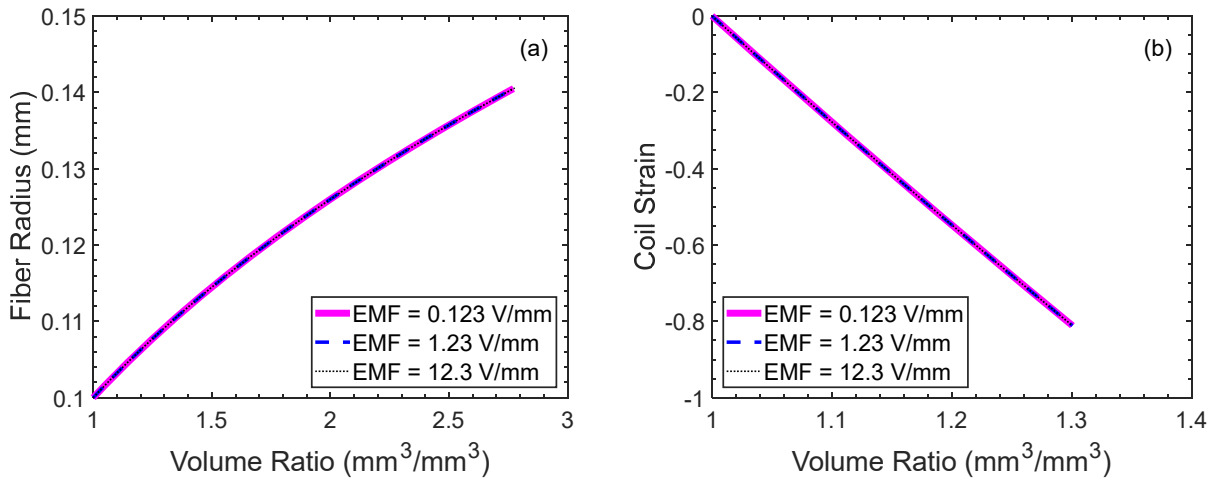

Figure S3. (a) Fiber radius versus volume ratio demonstrating that regardless of rate of actuation the 1/3 power dependence of radius on volume ratio is maintained. This is inherent in the model, and presented here for visualization purposes. (b) Coil strain versus volume ratio for three magnitudes of electric field demonstrates that the electric field does not affect the amount of swelling, but only the rate of swelling. For the parameters used in this study and over the range of swelling examined the coil strain has an approximately linear response to volumetric swelling. Note that the full range of swelling is not accessed in (b) due to coil-coil contact.

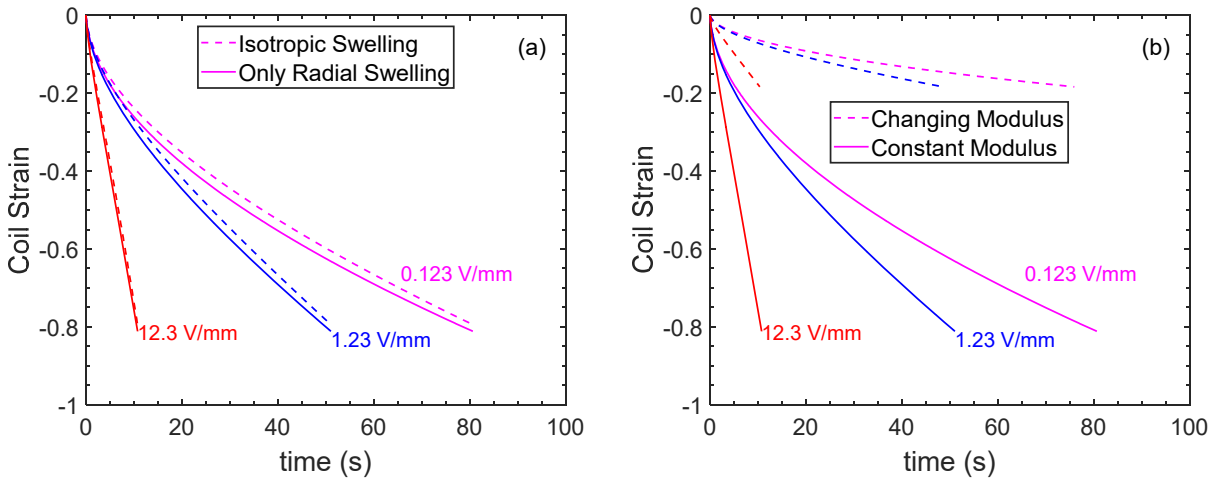

Figure S4. (a) Time-resolved coil strain demonstrating the benefit of anisotropic swelling (as reported in the main manuscript) as compared to isotropic swelling in which there is a small penalty (2.5%) due to increasing fiber length. **(b)** Time-resolved coil strain for a constant modulus fiber in which coil actuation is caused purely by increasing radius of the fiber (as reported in the main manuscript) compared to the case in which the modulus decreases with network swelling due to the density of crosslinks decreasing.

In Figure S4, the final coil strain at which coils come into contact is -0.811 for anisotropic swelling only in the radial direction, for the coil parameters reported in the main manuscript. If the fiber also swells axially, the final coil strain is reduced to -0.794, as shown in Figure S4a. For an ideal elastomer, the network modulus is proportional to the polymer density. Thus, the modulus decreases inversely with volume ratio.

$$E(t) = \frac{E(0)}{V_{ratio}}$$

In contrast to the R^2 dependence of $cos\beta$ in equation 37b, with changing modulus $cos\beta$ decreases more weakly with fiber radius, according to scaling arguments decreasing with the square root of fiber radius for an ideal elastomer.

$$cos\beta = \left| nR(t)^{1/2} \sqrt{\frac{\pi E(0) R(0)^3}{\mathbf{F}}} - 5 \right|$$

$E(0)$ and $R(0)$ are the initial, unswollen values. As shown in Figure S4b, the final coil strain for the parameters of this study decrease from -0.811 for constant modulus to -0.183 for a network modulus that decreases with swelling. As discussed in the main manuscript, the non-constant modulus coil strain is on par with that reported in literature for experiments. This study demonstrates the nearly order of magnitude enhancement in TCA actuation that can be achieved by incorporating a rigid core or other composite material in which the bending stiffness of the fiber is dictated by a nonswelling component and a swelling component causes increase in fiber radius.[3]

Supporting Information References

1. S. B. Harogoppad and T. M. Aminabhavi, *Macromolecules*, 1991, **24**, 2598-2605, DOI: 10.1021/ma00009a070.
2. S. B. Harogoppad and T. M. Aminabhavi, *Polymer*, 1990, **31**, 2346-2352, DOI: https://doi.org/10.1016/0032-3861(90)90323-Q.
3. C. Lamuta, S. Messelot and S. Tawfick, *Smart Materials and Structures*, 2018, **27**, 055018, DOI: 10.1088/1361-665X/aab52b.